

Received: 05.04.2023

Accepted: 12.07.2023

Research Article

*Theoretical kinetic investigation of the multichannel mechanism of O(<sup>3</sup>P) atmospheric oxidation reaction of but-3-enal*

Messaoudi Boulanouar<sup>a,b,1</sup>, Cheriet Mouna<sup>c</sup>, Djemil Rayenne<sup>d</sup>, Khatmi Djamel Eddine<sup>e</sup>

<sup>a</sup>Ecole Supérieure en Sciences Appliquées de Tlemcen, ESSA-Tlemcen, BP 165 RP Bel Horizon, Tlemcen 13000, Algeria

<sup>b</sup>Laboratory of Toxicomed, University of Tlemcen, P.O. Box 119, Tlemcen, 13000, Algeria

<sup>c</sup>Medicinal plants research unit (URPM.3000, Laghouat) attached to the biotechnology research center (CRBt 2500, Constantine), Constantine, Algeria

<sup>d</sup>Laboratory of Computational Chemistry and Nanostructures, University May 8, 1945, P.O. Box 401, Guelma, 24000, Algeria

<sup>e</sup>Aix Marseille Univ., CNRS, Centrale Marseille, iSm2, Marseille, France

**Abstract:** Several levels of theory such as Møller-Plesset MP2, G3, and CBS-QB3, have been used in order to investigate the complex and multichannel potential energy surface of the reaction of but-3-enal with the triplet oxygen atom. The results show that the O-addition channel is dominant. The different possible pathways of oxygen atom attack are thoroughly studied to better understand and explain the reaction mechanism. Regarding the oxidation of but-3-enal by triplet oxygen O(<sup>3</sup>P), it is shown that the major thermodynamic product is H<sub>3</sub>CC(O)CH<sub>2</sub>C(O)H (P3) being the most stable for the whole reaction. However, the most favored product kinetically is H<sub>2</sub>CC(OH)CH<sub>2</sub>C(O)H (P2). For the H-abstraction second possible pathway, the most favored product both kinetically and thermodynamically is found to be P8. The activation energy and calculated rate constants are consistent with the proposed addition mechanism.

**Keywords:** But-3-enal, O(<sup>3</sup>P), G3 method, O-addition, H-abstraction.

## 1. Introduction

Atmospheric chemical reactions have important characteristics for the environment. Various active species in the atmosphere, such as OH and NO<sub>3</sub> radicals, O<sub>3</sub> molecules, Cl and O(<sup>3</sup>P) atoms react with unsaturated compounds [1,2].

Atomic oxygen plays a very important role in the initial stages of the combustion of unsaturated hydrocarbons [3]. The theoretical approach used to explore the reaction paths allows a better understanding of the reaction mechanisms. Thus, it improves combustion efficiency [4-8].

Aldehydes have a significant importance and are widely used and employed in industrial process. They can be used as solvents, intermediates in dyes manufacturing, plastics, and even pharmaceuticals.

Aldehydes emission results from the incomplete combustion of hydrocarbons and other organic material such as fuel burning and can be biogenic resulting from photochemical reactions. Chemical degradation of the aldehyde compounds in the atmosphere leads to a variety of secondary pollutants. The resulting compounds of the reactions of these highly reactive unsaturated compounds present a significant impact on the air quality and can be harmful. It has been cited that the unsaturated aldehydes are more toxic than the saturated ones [9-11].

The atmospheric reactions of unsaturated aldehydes with triplet oxygen are characterized firstly by the O-addition mainly to the carbon-carbon double bond [12,13]. This step consists of an attachment of

<sup>1</sup> Corresponding Authors

e-mail: [messaoudiboulanouar@gmail.com](mailto:messaoudiboulanouar@gmail.com)

the electrophilic oxygen atom to the less substituted carbon atom of the double bond, forming an O-addition product. The addition of an O(<sup>3</sup>P) atom to the olefinic carbon yielding a triplet biradical has been suggested to be the key step for the reaction [4-8].

There are several experimental and modeling studies on O(<sup>3</sup>P) addition to aldehydes and unsaturated aldehydes. For instance, Gaffney et al. have determined the rate constants for the gas phase reaction of O(<sup>3</sup>P) atoms with selected unsaturated aldehydes and some other compounds relative to that for the reaction of O(<sup>3</sup>P) atoms with cyclopentene at 296±2K using a competitive technique. They have obtained the rate constants of crotonaldehyde relative to cyclopentene as unity. They have also compared and discussed rate constants for crotonaldehyde with existing literature values [14,15].

Passos et al. have obtained the thermal rate coefficients for the hydrogen abstraction reactions of but-3-enal by hydrogen. They have found that the abstraction reactions of but-3-enal proceed via five possible reaction channels. They have done a conformational search that leads to more than forty different structures of transition states. The activation energy estimation has shown strong temperature dependence [16].

Moreover, Atkinson et al. have determined relative rate constants for the reaction of some unsaturated carbonyls with OH radicals at 299 ± 2 K. Using a rate constant for the reaction of OH radicals with propene of  $2.52 \times 10^{-11} \text{ cm}^3\text{molecule}^{-1}\text{s}^{-1}$ , the rate constants obtained are crotonaldehyde,  $3.50 \pm 0.40$ ; and methylvinylketone,  $1.88 \pm 0.14$ . Their obtained data have been discussed and compared with literature values [17]. In another research paper for the same author, Atkinson et al. determined the rate constants for the gas-phase reactions of NO<sub>3</sub> radicals with a series of α,β-unsaturated aldehydes at 298 ± 2 K using a relative rate technique. Using rate constants for the reactions of NO<sub>3</sub> radicals with ethene and propene of  $(1.1 \pm 0.5) \times 10^{-16} \text{ cm}^3\text{molecule}^{-1}\text{s}^{-1}$  and  $(7.5 \pm 1.6) \times 10^{-15} \text{ cm}^3\text{molecule}^{-1}\text{s}^{-1}$ , respectively, they have obtained the rate constant of crotonaldehyde to be  $41 \pm 9$  (in units of  $10^{-16} \text{ cm}^3\text{molecule}^{-1}\text{s}^{-1}$ ) [18].

Papagni et al. measured the rate constants for the reactions of a series of aldehydes with OH and NO<sub>3</sub>

radicals at 296 ± 2 K. The rate constants obtained for the OH radical reactions were of the order of  $10^{-12} \text{ cm}^3\text{molecule}^{-1}\text{s}^{-1}$  by taking the methyl vinyl ketone as a reference. However, using methacrolein and 1-butene as the reference compounds, the rate constants for the NO<sub>3</sub> radical reactions having the order of  $10^{-15} \text{ cm}^3\text{molecule}^{-1}\text{s}^{-1}$  were obtained for propanal, butanal, pentanal, and hexanal, respectively. They have found that the reaction with the OH radical is the dominant loss process [19].

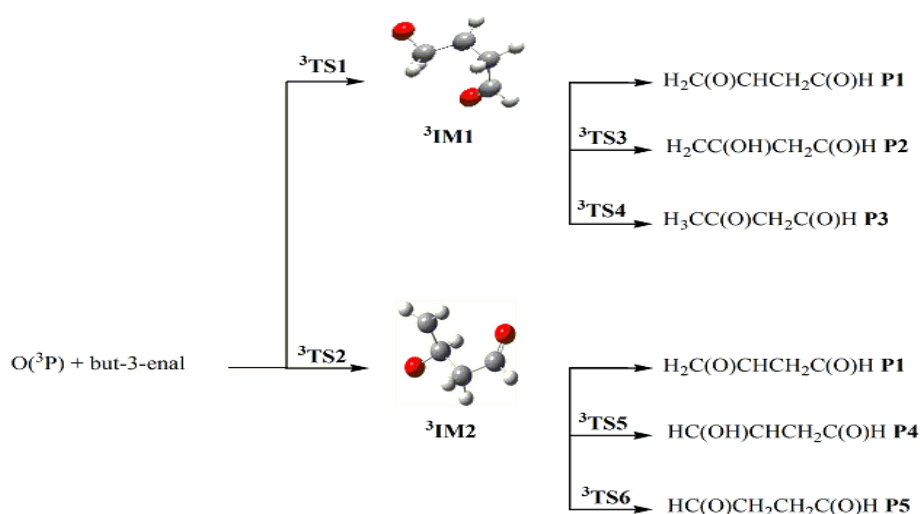
Atkinson et al. have studied the rate constants for the reactions of O<sub>3</sub> with some ketones and aldehydes at the gas phase at 296 ± 2 K. They have also discussed the substituent effects of CHO and CH<sub>3</sub>CO groups on the rate constants [20].

Grosjean et al. have investigated the kinetics of the reaction of O<sub>3</sub> with some unsaturated oxygenated compounds (alcohols, carbonyls, and esters) in the air at ambient temperature (285–295 K) and atmospheric pressure. In addition, they have discussed the substituent effects on the reactivity of unsaturated alcohols with respect to alkenes [21].

The study of the oxidation mechanism of but-3-enal and its kinetics is very important and provides a fruitful contribution to the best understanding of the hierarchical development of hydrocarbon combustion. This paper aims to perform a theoretical study of the different reaction channels of the reaction of O(<sup>3</sup>P) with but-3-enal by exploring several calculations at the MP2, G3, and CBS-QB3 levels of theory. Both oxidation and H-abstraction channels of but-3-enal by triplet oxygen O(<sup>3</sup>P) are explored in detail along with the triplet potential energy surface. The major products of these reactions are predicted and localized. Thermal rate constants for the O(<sup>3</sup>P) + but-3-enal were determined over the temperature range 298-798 using transition state theory (TST) [22,24].

## 2. Computational Method

The Gaussian 09 program [25] and the 2nd order perturbation Møller-Plesset theory (MP2) [26] with the basis set 6-31G (d), complete basis set (CBS) methods G3 [27,28] and CBS-QB3 [29,30] were used to carry out calculations. Geometry optimizations followed by frequency calculations for all reactants, products, and transition states (TS) of the addition of triplet oxygen O(<sup>3</sup>P) on but-3-enal were performed at the same level of theory.



**Scheme 1.** Schematic representation of the different O-addition paths of the studied reaction of but-3-enal with  $O(^3P)$ .

**Table 1.** Thermodynamic properties  $\Delta H$  (kcal/mol),  $\Delta G$  (kcal/mol) and  $\Delta S$  (cal/molK) of reactants, products, intermediates and transition states calculated by MP2/6-31G(d), G3 and CBS-QB3 methods.

		MP2/6-31G(d)			G3			CBS-QB3		
		$\Delta H$	$\Delta G$	$\Delta S$	$\Delta H$	$\Delta G$	$\Delta S$	$\Delta H$	$\Delta G$	$\Delta S$
<b>But-3-enal + <math>O(^3P)</math></b>		0.0	0.0	0.0	0.0	0.0	0.0	0.0	0.0	0.0
<b><math>H_2C(O)CHCH_2C(O)H</math></b>	<b>P1</b>	-85.4	-75.8	-32.3	-85.9	-76.2	-32.9	-87.5	-77.8	-32.5
<b><math>H_2CC(OH)CH_2C(O)H</math></b>	<b>P2</b>	-97.6	-87.8	-32.9	-103.9	-94.2	-32.9	-104.7	-95.1	-32.3
<b><math>H_3CC(O)CH_2C(O)H</math></b>	<b>P3</b>	-116.0	-107.0	-30.3	-115.3	-106.4	-30.1	-116.2	-107.3	-29.9
<b><math>HC(OH)CHCH_2C(O)H</math></b>	<b>P4</b>	-92.6	-83.9	-29.3	-99.7	-91.1	-29.3	-100.6	-91.7	-29.6
<b><math>HC(O)CH_2CH_2C(O)H</math></b>	<b>P5</b>	-112.6	-102.9	-32.7	-111.7	-102.2	-32.2	-112.8	-103.5	-31.3
<b><math>^3IM1</math></b>		-20.5	-12.3	-27.4	-25.8	-17.9	-27.0	-26.8	-18.9	-26.8
<b><math>^3IM2</math></b>		-21.4	-12.6	-29.3	-26.3	-17.7	-29.2	-26.7	-18.7	-27.0
<b><math>^3TS1</math></b>		11.2	19.6	-28.3	5.7	13.9	-28.2	-1.2	6.9	-27.1
<b><math>^3TS2</math></b>		12.3	20.1	-26.0	1.6	9.2	-25.8	0.1	7.4	-24.4
<b><math>^3TS3</math></b>		9.3	18.3	-29.9	0.5	9.0	-29.3	-0.4	8.3	-29.2
<b><math>^3TS4</math></b>		16.0	25.1	-30.5	3.8	12.7	-30.4	1.8	10.7	-30.1
<b><math>^3TS5</math></b>		14.5	22.1	-25.6	3.9	11.5	-26.0	2.8	10.3	-25.1
<b><math>^3TS6</math></b>		19.3	27.6	-28.0	6.5	15.0	-28.8	4.3	12.6	-27.8

An IRC (Intrinsic reaction coordinate) calculation is necessary to perform and verify that the optimized structure is representative of the desired reaction coordinate [31]. With the IRC result, the structures of transition states are checked whether they connect the two minima. The rate constants for the gas-phase reaction of atom oxygen with but-3-enal were also calculated using non-adiabatic transition state theory (TST) over the temperature range of 298-798K.

### 3. Results and discussion

The reaction of  $O(^3P)$  with but-3-enal leads to two primarily possible pathways; O-addition and H-abstraction.

#### 3.1. O-Addition to but-3-enal

The O-addition to the but-3-enal leads to a variety of several products as it is shown in Scheme 1.

The obtained values of enthalpy, Gibbs free energy, and entropy are given in Table 1 for all the optimized structures corresponding to the O-addition at different levels of theory.

The relative free enthalpies and enthalpies of P1, P2, P3, P4, and P5 calculated by MP2 and G3

methods are negative. This shows that the triplet oxygen addition reaction  $O(^3P)$  on but-3-enal is spontaneous and exothermic.

The obtained calculations by the methods MP2 and G3 summarized in Table 1 show that the bi-ketone products P3 and P5 are the most stable.

From an energetic point of view, the  $O(^3P)$  atom addition can occur on either carbon atom of the double bond.

Figure 1 shows the potential energy profile of the triplet reaction paths for the possible addition pathways calculated at the G3 theory for the  $O(^3P)$  reaction with but-3-enal at 298.15K as a function of Gibbs's free energy changes. The structures of intermediates and different transition states are also presented in this figure.

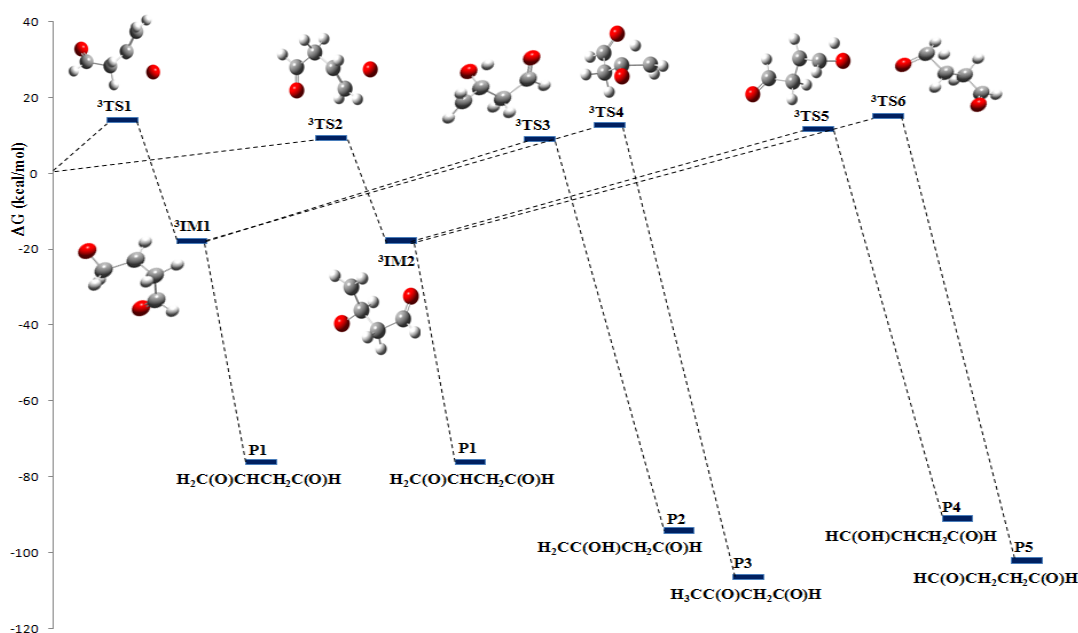
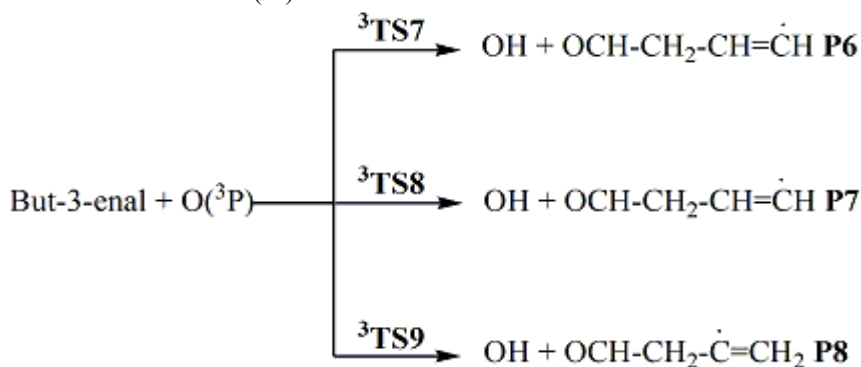


**Figure 1.** Energetic profile in kcal/mol of the different channels for the reaction pathways addition of but-3-enal with  $O(^3P)$  which is calculated at G3 level at 298.15 K.



**Scheme 2.** Schematic representation of the three possible H-abstraction channels of but-3-enal by oxygen atom.

In Figure 1, the first transition state  $^3TS1$  located at 13.9 kcal/mol is higher in energy than the isolated reactants and corresponds to the  $O(^3P)$  addition to but-3-enal. This leads to the intermediate  $^3IM1$  ( $\text{CH}(\text{O})\text{CH}_2\text{CHCH}_2(\text{O})$ ) formation, which is located at -17.9 kcal/mol.

Three reaction pathways follow the formation of this triplet adduct. As a first reaction channel, the

intermediate  $^3IM1$  could rearrange to give rise to the formation of epoxy product P1 ( $\text{H}_2\text{C}(\text{O})\text{CHCH}_2\text{C}(\text{O})\text{H}$ ), which is located at -76.2 kcal/mol. This cyclic compound is obtained by closing the three-membered cycle at the C-O bond level. The C-O bond shortens from 2.392Å in  $^3IM1$  to 1.436Å in product P1.

The product P2 ( $\text{H}_2\text{CC}(\text{OH})\text{CH}_2\text{C}(\text{O})\text{H}$ ) with an energy of 94.2 kcal/mol below the reactants is formed by the second energy path, with a barrier of 26.9 kcal/mol between  $^3\text{IM1}$  and  $^3\text{TS3}$ , via  $^3\text{TS3}$  located at 9.0 kcal/mol showing an imaginary frequency of  $2583.5\text{icm}^{-1}$ . It is worth noting that  $^3\text{TS3}$  results from forming the (C = O) bond and breaking (C-H) bond of the C4 carbon from  $^3\text{IM1}$ . This path channel corresponds to the rearrangement of lower energy from  $^3\text{IM1}$ , which makes P2 the main product.

The third path corresponding to the least energetic channel leads to the product P3 ( $\text{H}_3\text{CC}(\text{O})\text{CH}_2\text{C}(\text{O})\text{H}$ ) located at -106.4 kcal/mol. P3, to get formed, has to overcome  $^3\text{TS4}$  with a barrier of 12.7 kcal/mol relative to the reactants and an imaginary frequency of  $2577.8\text{icm}^{-1}$ .

Moreover, the intermediate  $\text{CH}(\text{O})\text{CH}_2\text{CH}(\text{O})\text{CH}_2$  ( $^3\text{IM2}$ ), which corresponds to the O-addition to the more substituted carbon of the but-3-enal double bond, is located at -17.7 kcal/mol via  $^3\text{TS2}$  characterized by a barrier of 9.2 kcal/mol. This intermediate  $^3\text{IM2}$  could form the product P4 ( $\text{HC}(\text{OH})\text{CHCH}_2\text{C}(\text{O})\text{H}$ ), which is located at 91.1 kcal/mol below the reactants via  $^3\text{TS5}$  with an imaginary frequency of  $2604.1\text{icm}^{-1}$  and a barrier of 11.5 kcal/mol. In addition, product P5 ( $\text{HC}(\text{O})\text{CH}_2\text{CH}_2\text{C}(\text{O})\text{H}$ ) could also be formed by  $^3\text{IM2}$ . It is located at -102.2 kcal/mol and surpasses  $^3\text{TS6}$ , which is 15.0 kcal/mol relative to reactants. This transition state presents an imaginary frequency of  $2597.7\text{icm}^{-1}$ .

### 3.2. H-abstraction

The general scheme of the possible H-abstraction reactions from but-3-enal by the triplet oxygen atom is summarized in Scheme 2.

From this scheme, it can be seen that three possible H-abstraction can take place. The triplet oxygen atom can abstract either of the hydrogens of the terminal carbon of the double bond in but-3-enal. These two hydrogen atoms are symmetrical and the only difference between them is that one is on the top of the double bond and the second one at the bottom depending on the side of the oxygen attack. The third hydrogen belongs to the second carbon atom of the double bond in the molecule.

The obtained values of enthalpy, Gibbs free energy, and entropy at different levels of theory are given in Table 2.

As it is shown in Figure 2 and Scheme 2, three H-abstraction possible channels are found for the but-3-enal once attacked by  $\text{O}(^3\text{P})$ .

Firstly, the oxygen atom attack to the first side H atom of the double bond gives rise to the product P6 ( $\text{OH} + \text{CH}_2=\text{CH}-\text{CH}=\text{CH}$ ) with a stabilization energy of 6.1 kcal/mol via the transition state  $^3\text{TS7}$  located at 17.4 kcal/mol above reactants with an imaginary frequency of  $2927.4\text{icm}^{-1}$ . The second one, when the oxygen atom attacks the second side H atom of the double bond leading to the product P7 ( $\text{OH} + \text{CH}_2=\text{CH}-\text{CH}=\text{CH}$ ), 6.3 kcal/mol above reactants, via the transition state  $^3\text{TS8}$  located at 17.4 kcal/mol. The imaginary frequency of this TS is  $2930.2\text{icm}^{-1}$ . The last possible H-abstraction product P8 ( $\text{OH} + \text{CH}_2=\text{CH}-\text{C}=\text{CH}_2$ ) is located at 2.7 kcal/mol and is then formed via the transition state  $^3\text{TS9}$  lying on 14.7 kcal/mol characterized by the imaginary frequency  $2919.6\text{icm}^{-1}$ . Among the three products of the H-abstraction, the P8 product is the most favored kinetically and thermodynamically.

In summary, for the overall reaction and according to the thermochemical results, the dominant reaction channel for this PES is the electrophilic O-addition. Moreover, the kinetically determining stages are the first paths of addition of oxygen atoms to but-3-enal.

### 3.3. Reaction rate calculation

Characterizing the dominant elementary reaction is the key to understand the overall reaction mechanism. Among the theories used to achieve this goal, we can cite TST.

Transition State Theory aims to provide a mathematical expression for the rate constants of elementary reactions. Under these conditions, the rate constant  $k$  is given by Eyring's equation [22-24]:

$$k = \frac{k_B T}{h} \exp\left(-\frac{\Delta G^\ddagger}{RT}\right) \sigma$$

$\Delta G^\ddagger$  is the free energy variation at the transition state and expressed as  $\Delta G^\ddagger = G^\circ(\text{TS}) - \Sigma G^\circ(\text{reactants})$ ,  $T$  is the temperature (K),  $h$  is Planck's constant,  $k_B$  is Boltzmann's constant, and  $R$  is the gas constant.

As shown in the above equation, we have used one-dimensional Eckart tunneling correction to improve the rate constants of the studied reaction by using a multiplicative coefficient.

The tunnel effect is simply the rate constant multiplied by the transmission coefficient  $\sigma(T)$ . This latter depends on the temperature, the mass of the particle, and the shape of the energy barrier between reactants and products. If the tunnel effect is neglected, then  $\sigma(T) = 1$ .

Singleton and Cvetanović [32] have used a simple expression based on transition state theory TST to calculate the rate constant  $k(T)$  of  $O(^3P) +$  olefin reactions below 500 K.

To calculate the rate constants of reactions at the temperature range of 298–798 K, the KiSThelP program [33-35] has been used based on the molecular properties of reactants, transition states, and products calculated at the MP2 method at the 6-

31G (d) basis set. The results are shown in Figure 3 and compared to the results obtained by Adusei et al. [36].

### 3.3.1. O-addition reaction

The rate constant of reactions R1 and R2 are lower than any other paths at the temperature range of 298–798K.

Arrhenius plots for the reactions of but-3-enal with  $O(^3P)$  derived from the obtained data are shown in Figure 3. Unweighted linear least-squares analysis of these data gives to the following Arrhenius expressions.

**Table 2.** Thermodynamic properties  $\Delta H$  (kcal/mol),  $\Delta G$  (kcal/mol) and  $\Delta S$  (cal/molK) of reactants, products and transition states for the H-abstraction channels calculated by MP2/6-31G (d), G3 and CBS-QB3 methods.

	MP2/6-31G(d)			G3			CBS-QB3		
	$\Delta H$	$\Delta G$	$\Delta S$	$\Delta H$	$\Delta G$	$\Delta S$	$\Delta H$	$\Delta G$	$\Delta S$
But-3-enal + $O(^3P)$	0.0	0.0	0.0	0.0	0.0	0.0	0.0	0.0	0.0
OH + HC(O)CH <sub>2</sub> CH=CH P6	24.3	23.7	27.4	8.3	6.1	7.6	8.9	6.7	7.5
OH + HC(O)CH <sub>2</sub> CH=CH P7	24.7	24.2	27.5	8.6	6.3	7.7	9.2	7.0	7.5
OH + HC(O)CH <sub>2</sub> C=CH <sub>2</sub> P8	21.3	20.6	28.21	5.2	2.7	8.3	5.6	3.1	8.2
<sup>3</sup> TS7	26.8	34.3	-25.1	10.5	17.4	-23.8	9.7	16.9	-24.4
<sup>3</sup> TS8	27.5	34.8	-24.2	10.7	17.4	-23.0	9.7	16.6	-23.2
<sup>3</sup> TS9	24.3	31.7	-25.1	7.8	14.7	-23.6	7.1	4.3	-24.2

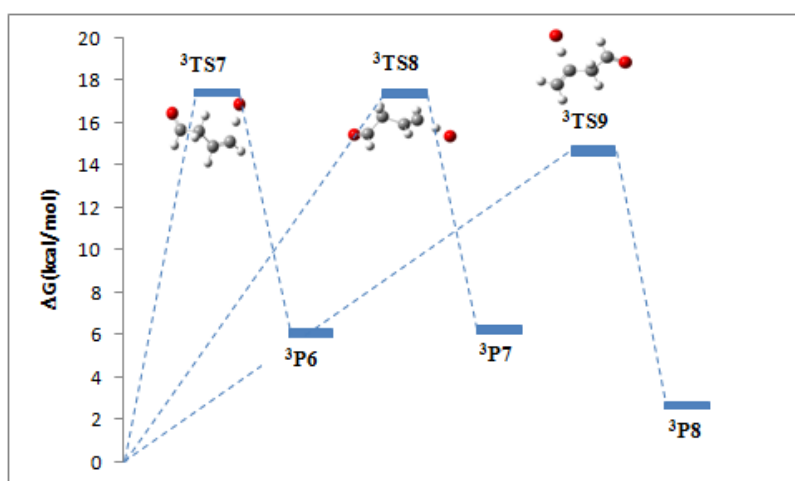


**Figure 2.** Energetic profile in kcal/mol of the three possible H-abstraction channels of but-3-enal with  $O(^3P)$  at G3 level at 298.15 K.

Messaoudi Boulanouar, Cheriet Mouna, Djemil Rayenne, Khatmi Djamel Eddine

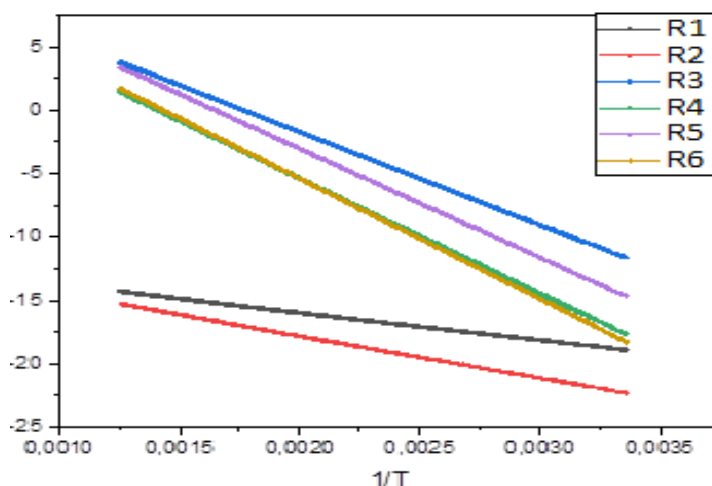


Figure 3. Arrhenius plots for the addition reaction of O(<sup>3</sup>P) to but-3-enal in the range of 298-798K calculated at the MP2 level of theory.

Table 3. Arrhenius expressions of rate constants (in units of cm<sup>3</sup>. molecule<sup>-1</sup>. s<sup>-1</sup>) of the O-addition channels to but-3-enal.

k(T)	Aexp(-E <sub>a</sub> /RT)	A T <sup>n</sup> exp(-E <sub>a</sub> /RT)
k <sub>1</sub>	2.526 x 10 <sup>-12</sup> exp (-41.95/RT)	9.431 x 10 <sup>-17</sup> T <sup>1.41</sup> exp (-36.30/RT)
k <sub>2</sub>	7.375 x 10 <sup>-12</sup> exp (-63.94/RT)	5.16 x 10 <sup>-16</sup> T <sup>1.31</sup> exp (-58.69/RT)
k <sub>3</sub>	9.662 x 10 <sup>12</sup> exp (-140.68/RT)	1.337 x 10 <sup>09</sup> T <sup>1.23</sup> exp (-135.76/RT)
k <sub>4</sub>	6.419 x10 <sup>12</sup> exp (-173.97/RT)	3.864x 10 <sup>09</sup> T <sup>1.03</sup> exp (-169.86/RT)
k <sub>5</sub>	1.469 x10 <sup>14</sup> exp (-164.56/RT)	5.947 x 10 <sup>12</sup> T <sup>0.44</sup> exp (-162.79/RT)
k <sub>6</sub>	3.623 x 10 <sup>13</sup> exp (-181.72/RT)	1.054x 10 <sup>13</sup> T <sup>0.17</sup> exp (-181.04/RT)

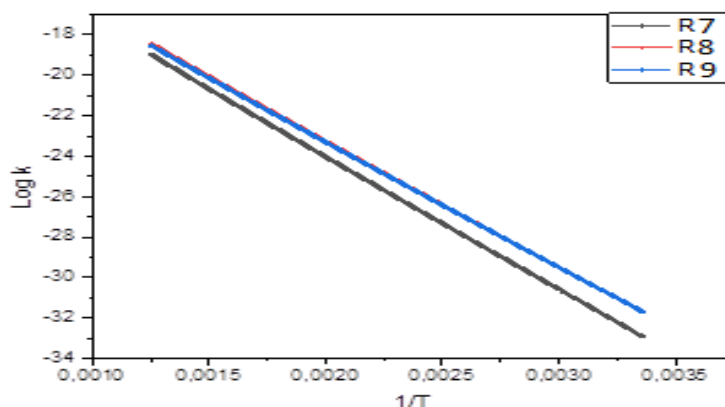


Figure 4. Arrhenius plots for the H-abstraction reaction of but-3-enal with O(<sup>3</sup>P) in the range of 298-798 K calculated at the MP2 level of theory.

Table 4. Arrhenius expressions of rate constants (in units of cm<sup>3</sup>. molecule<sup>-1</sup>. s<sup>-1</sup>) of the H-abstraction channels of but-3-enal.

k(T)	Aexp(-E <sub>a</sub> /RT)	A T <sup>n</sup> exp(-E <sub>a</sub> /RT)
k <sub>7</sub>	1.781 x 10 <sup>-11</sup> exp (-117.99/RT)	2.725 x 10 <sup>-18</sup> T <sup>2.17</sup> exp (-117.99/RT)
k <sub>8</sub>	2.801 x 10 <sup>-11</sup> exp (-120.92/RT)	5.185 x 10 <sup>-18</sup> T <sup>2.15</sup> exp (-112.34/RT)
k <sub>9</sub>	1.841 x 10 <sup>-11</sup> exp (-119.81/RT)	2.560 x 10 <sup>-18</sup> T <sup>2.19</sup> exp (-111.07/RT)

The results given in table 3 show that k<sub>1</sub> and k<sub>2</sub> are lower than the other rate constants at the same

temperature. This means that the corresponding two reactions are kinetically determining steps.

### 3.3.2. H-abstraction reaction

The H-abstraction is a significant reaction since it includes the reaction channels R7, R8, and R9. The calculated rate constants of the H-abstraction reaction are shown in Figure 4.

For the reactions R7, R8, and R9, the rate constants calculated from the quantum chemistry calculation using MP2 are highly consistent. The temperature dependence expressions of rate constants for these reactions are given in Table 4.

Table 4 shows that the values of the activation energies of the three reactions are so close and can be seen very well on the Arrhenius plots.

We can therefore see that despite the absence of experimental work on the oxidation of but-3-enal from a kinetic point of view, the O-addition dominates in the temperature range studied and its first two steps are kinetically determining.

## 4. Conclusions

In the present work, different reaction channels for the reaction between  $O(^3P)$  and but-3-enal are probed at the MP2, G3, and CBS-QB3 levels of theory. The obtained structures were well reproduced by the calculation of the reaction paths IRC.

Our theoretical approach was used to explore the reaction paths and allow a better understanding of the reaction mechanism.

The thermodynamic study carried out by calculating the thermodynamic parameters such as;  $\Delta H$  and  $\Delta G$  shows that the oxidation reaction of but-3-enal is exothermic and could occur spontaneously under the condition of 1atm and 298K. The dominant reaction channel for this PES is the electrophilic O-addition to but-3-enal one characteristic double bond. The values of Gibbs free energy confirm that the formation of the P3 product is the most thermodynamically stable reaction product. The activation energy values show that P2 is the most favored thermodynamically.

For the H-abstraction, product P8 is found to be the most favored one thermodynamically and kinetically, whereas products P6 and P7 are less favored with equivalent stability order.

Rate coefficients for consumption of ground-state oxygen atom by reaction with but-3-enal have been determined using Transition State Theory. In fact, the first two O-addition pathways are the kinetically

determining steps; the activation energy is consistent with the addition mechanism proposed.

The obtained results support the dominance of the electrophilic O-addition mechanism on the double bond under the temperature range studied. The obtained findings are in good commitment with the experimental reaction rate under the range of temperature 298-798 K studied.

## ACKNOWLEDGEMENT

The authors would like to thank the Ministry of Higher Education and Scientific Research, Algeria, for its fruitful support.

## References

- [1] R. Atkinson, "Gas-phase tropospheric chemistry of organic compounds: a review," *Atmospheric Environment. Part A. General Topics*, 24 (1990) 1-41.
- [2] B. J. Finlayson-Pitts, J. N. Pitts Jr, "Chemistry of the upper and lower atmosphere" San Diego, CA: Academic (2000).
- [3] A. Caracciolo, G. Vanuzzo, N. Balucani, et al., "Combined experimental and theoretical studies of the  $O(^3P) + 1$ -butene reaction dynamics: Primary products, branching fractions, and role of intersystem crossing," *The Journal of Physical Chemistry A*, 123 (2019) 9934-9956.
- [4] C. Cavallotti, A. Della Libera, C. W. Zhou, et al., "Crossed-beam and theoretical studies of multichannel nonadiabatic reactions: branching fractions and role of intersystem crossing for  $O(^3P) + 1,3$ -butadiene," *Faraday Discussions*, 238 (2022) 161-182.
- [5] J. F. Alarcon, A. M. Mebel, "Direct H abstraction by molecular oxygen from unsaturated C3-C5 hydrocarbons: A theoretical study," *International Journal of Chemical Kinetics*, 54 (2022) 203-217.
- [6] R. Quandt, M. Zhiyuan, W. Xuebin, et al., "Reactions of  $O(^3P)$  with alkenes: H,  $CH_2CHO$ , CO, and OH channels," *The Journal of Physical Chemistry A*, 102 (1998) 60-64.
- [7] S. Hirokami, R. J. Cvetanović, "Reaction of oxygen atoms,  $O(^3P)$ , with olefins in liquid nitrogen solution at 770K," *Journal of the American Chemical Society*, 96 (1974) 3738-3746.
- [8] T. Oguchi, I. Akira, K. Yukino et al., "Mechanism of the reactions of butenes with  $O(^3P)$ : the yields of  $CH_3$  and  $C_2H_5$ ," *The Journal*

- of Physical Chemistry A, 108 (2004) 1409-1416.
- [9] Y. Ren, L. Zhou, A. Mellouki, et al., "Reactions of NO<sub>3</sub> with aromatic aldehydes: gas-phase kinetics and insights into the mechanism of the reaction," *Atmospheric Chemistry and Physics*, 21 (2021) 13537-13551.
- [10] B. Long, Y. Xia, D. G. Truhlar, "Quantitative kinetics of HO<sub>2</sub> reactions with aldehydes in the atmosphere: high-order dynamic correlation, anharmonicity, and falloff effects are All important," *Journal of American Chemical Society*, 144 (2022) 19910-19920.
- [11] C. N. Hewitt, "Reactive Hydrocarbons in the Atmosphere, Academic Press, (1998).
- [12] C.A. Taatjes, H. Nils, M. Andrew, et al., "Enols are common intermediates in hydrocarbon oxidation," *Science*, 308 (2005) 1887-1889.
- [13] Z. Min, W. Teh-Hwa, S. Hongmei, et al., "Reaction of O(<sup>3</sup>P) with alkenes: Side chain vs double bond attack," *The Journal of Physical Chemistry A*, 104 (2000) 9941-9943.
- [14] J. S. Gaffney, R. Atkinson, J. N. Pitts Jr., "Relative rate constants for the reaction of oxygen (<sup>3</sup>P) atoms with selected olefins, monoterpenes, and unsaturated aldehydes," *Journal of the American Chemical Society*, 97 (1975) 5049-5051.
- [15] J. S. Gaffney, R. Atkinson, N. Pitts Jr. James, "Temperature dependence of the relative rate constants for the reaction of oxygen (<sup>3</sup>P) atoms with selected olefins, monoterpenes, and unsaturated aldehydes," *Journal of the American Chemical Society*, 97 (1975) 6481-6483.
- [16] M. Passos, L. Igor, V. Mateus, et al., "The 3-butenal+ H reactions: an application of the multipath canonical variational theory," *Authorea Preprints*, (2020).
- [17] R. Atkinson, M.A. Sara, N. Pitts Jr. James, "Kinetics of the gas-phase reactions of OH radicals with a series of  $\alpha$ ,  $\beta$ -unsaturated carbonyls at 299±2 K," *International Journal of Chemical Kinetics*, 15 (1983) 75-81.
- [18] R. Atkinson, "A structure-activity relationship for the estimation of rate constants for the gas-phase reactions of OH radicals with organic compounds," *International Journal of Chemical Kinetics*, 19 (1987) 799-828.
- [19] C. Papagni, A. Janet, R. Atkinson, "Rate constants for the gas-phase reactions of a series of C<sub>3</sub>- C<sub>6</sub> aldehydes with OH and NO<sub>3</sub> radicals," *International Journal of Chemical Kinetics*, 32 (2000) 79-84.
- [20] R. Atkinson, M. A. Sara, M.W. Arthur, et al., "Rate constants for the gas-phase reactions of O<sub>3</sub> with a series of carbonyls at 296 K," *International Journal of Chemical Kinetics*, 13 (1981) 1133-1142.
- [21] D. Grosjean, E. Grosjean, E. L. Williams, "Rate constants for the gas-phase reactions of ozone with unsaturated alcohols, esters, and carbonyls," *International Journal of Chemical Kinetics*, 25 (1993) 783-794.
- [22] P. Pechukas, "Transition state theory," *Annual Review of Physical Chemistry*, 32 (1981) 159-177.
- [23] B. L. Foley, A. Bhan, "Degree of rate control and De Donder relations—An interpretation based on transition state theory," *Journal of Catalysis*, 384 (2020) 231-251.
- [24] a) K. Han, T. Chi, "Reaction rate constant computations: theories and applications (Vol. 6)," *Royal Society of Chemistry*, (2014). b) B. Peters, "Reaction rate theory and rare events," *Elsevier*, (2017).
- [25] M. J. Frisch, G. W. Trucks, H. B. Schlegel, et al., *Gaussian 09, Inc., Wallingford CT*, 2009.
- [26] M. Head-Gordon, J. A. Pople, M. J. Frisch, "MP2 energy evaluation by direct methods," *Chemical Physics Letters*, 153 (1988) 503-506.
- [27] L. A. Curtiss, R. Krishnan, C. R. Paul, et al., "Gaussian-3 (G3) theory for molecules containing first and second-row atoms," *The Journal of Chemical Physics*, 109 (1998) 7764-7776.
- [28] L. A. Curtiss, R. Krishnan, "Gaussian-3 and related methods for accurate thermochemistry," *Theoretical Chemistry Accounts*, 108 (2002) 61-70.
- [29] G. A. Petersson, T. G. Tensfeldt, J. A. Montgomery Jr., "A complete basis set model chemistry. III. The complete basis set-quadratic configuration interaction family of methods," *Journal of Chemical Physics*, 94 (1991) 6091-6101.
- [30] J. W. Ochterski, G. A. Petersson, J. A. Montgomery Jr., "A complete basis set model chemistry. V. Extensions to six or more heavy

- atoms," *Journal of Chemical Physics*, 104 (1996) 2598-2619.
- [31] C. Gonzalez, H. B. Schlegel, "Reaction path following in mass-weighted internal coordinates," *Journal of Physical Chemistry*, 94 (1990) 5523-5527.
- [32] D. L. Singleton, R. J. Cvetanović, "Temperature dependence of the reaction of oxygen atoms with olefins," *Journal of the American Chemical Society*, 98 (1976) 6812-6819.
- [33] S. Canneaux, F. Bohr, E. Henon, "KiSThelP: a program to predict thermodynamic properties and rate constants from quantum chemistry results," *Journal of Computational Chemistry*, 35 (2014) 82-93.
- [34] H. Khartabil, L. Doudet, I. Allart-Simon, et al., "Mechanistic insights into Smiles rearrangement. Focus on  $\pi$ - $\pi$  stacking interactions along the radical cascade," *Organic & Biomolecular Chemistry*, 18 (2020) 6840-6848.
- [35] J. Dang, S. Tian, Q. Zhang, "Mechanism and kinetics studies of the atmospheric oxidation of *p*, *p'*-Dicofol by OH and NO<sub>3</sub> radicals," *Chemosphere*, 219 (2019) 645-654.
- [36] G. Y. Adusei, A. Fontijn, "Kinetics of the reaction between oxygen (<sup>3</sup>P) atoms and 1, 3-butadiene between 280 and 1015 K," *The Journal of Physical Chemistry*, 97 (1993) 1406-1408.